CHEMISTRY OF MATERIALS

COMMUNICATION

pubs.acs.org/cm

Growth of Carbon Nanotubes Catalyzed by Defect-Rich Graphite Surfaces

Jarrn H. Lin,*[,†] Ching S. Chen,[‡] Mark H. Rümmeli,[§,∥] Alicja Bachmatiuk,[§] Zhi Y. Zeng,[†] Hui L. Ma,[†,⊥] Bernd Büchner,[§] and Hsiu W. Chen*[,⊥]

[†]Dept. of Material Science, National University of Tainan, 33, Sec. 2, Shu-Lin Street, Tainan 70005, Taiwan

[‡]Center of General Education, Chang Gung University, 259 Wen-Hwa first Road, Kwei-shan, Tao-Yuan 333, Taiwan

[§]IFW Dresden, P.O. Box 270116, D-01171 Dresden, Germany

[∥]Technische Universität Dresden, Dresden, D-01062, Germany

[⊥]Department of Chemistry and Center for Nanoscience and Technology, National Sun Yat-sen University, 70 Lien Hai Road, Kaohsiung 80424, Taiwan

Supporting Information

KEYWORDS: carbon materials, chemical vapor deposition, characterization of materials

Carbon nanotubes (CNTs) have attracted a great deal of interest in academia and industry owing to their unique and novel physicochemical properties. This led to the development of various synthesis methods for their production. In particular many efforts focused on metal-assisted chemical vapor deposition (MA-CVD). However, a core shortcoming of the metal-assisted pathway is that the metallic nanoparticles used as catalysts usually contaminate the CNTs, forcing the need for postsynthesis purification. Although purification routes can remove most of the residual metal particles,[1−3] they usually cause structural defects limiting their use in applications. An alternative and more desirable approach is to grow CNTs directly on a substrate without further treatment being required. This has spurred the development of metal-free CVD for fabricating CNTs with high yield or at desired positions. Recent studies have demonstrated that metal-free catalytic routes can grow carbon nanotubes (CNTs). Cheng et al. and Huang et al. have successfully demonstrated the growth of single-walled CNTs (SWNTs) on silicon wafers without the aid of metal catalysts.[4,5] More interestingly, Takagi et al. presented straight growth of SWNTs on nanodiamond through a metal-free process and proposed a new model, the vapor−solid−surface−solid (VSSS), to explain the formation of SWNTs on diamond surfaces via metal-free chemical vapor deposition.[6] This model can be inferred from findings on the catalytic growth behaviors of SWNTs by the non-iron group metal catalysts, such as Au, Ag, and Cu.[7,8] However, the manner in which the dissociation of the carbon-bearing molecules are able to form CNTs over nonmetals is still an open question. Recently, Liu et al. suggested that the lift-off behavior of deposited carbon or graphite layers on nonmetals determines the growth of CNTs.[9] However, further experimental evidence for this concept is still required, especially the growth mechanism of CNTs catalyzed by a metal-free process. Here, we report that MWNTs can grow directly on defective graphite surfaces through CVD with helium diluted ethylene as the feedstock at 850 °C. We show various routes, acid treatment, oxygen oxidation, and laser ablation to induce that suitable defects are possible.

The growth of MWNTs was performed using flake graphite powder (Aldrich, purity > 99.99%) and highly oriented pyrolytic graphite (HOPG, grade ZYA from SPI Supplies Co.). To ensure no metal or unwanted nonmetal contaminants were present in the original samples or post-treated ones, various elemental characterization tools were employed, namely, energy dispersive spectroscopy (EDS) in a scanning and transmission electron microscope (SEM, JEOL JSM-6700F; TEM, JEOL AEM-2100), thermogravimetric analysis (TGA, TA Q500), and inductively coupled plasma mass spectrometry (ICP-MS, PE-SCIEX ELAN 6100 DRC). Elemental analyses for the pristine and post-treated samples were performed via this procedure: samples were subjected to combustion using TGA for tracing the ash content and then the ash was dissolved in concentrated nitric acid for ICP-MASS measurement. Micro- and nanoscale element distribution of samples was carried out by EDS equipped with TEM or SEM.

Prior to the CNT growth process, the graphite samples were subjected to three activation routes. These are oxygen oxidation, acid treatments, and laser ablation on the graphite to produce defects and oxygenated functional groups. The oxygen oxidation was conducted in a fixed bed reactor by introducing 2% oxygen to an Ar flow (40 mL/min) at 680 °C for 30 min. Acid treatment of the samples was carried out in a reflux system at 80 °C for 2 h in a 2 M HNO_3 solution. The laser ablation was conducted with a Nd:YAG laser (wavelength at 355 nm, power 30 mJ, pluse duration 5 ns, and beam diameter 6 mm) on a thin 5 × 5 mm^2 HOPG layer, which was radiated by the laser light for 10 pulses at several spots in 1 s in open air. The CVD route for the growth of the CNT was accomplished in a fixed bed quartz reactor at 850 °C for 30 min using a C_2H_4/He mixture at a ratio of 1/9 and a flow of 40 mL/min at atmospheric pressure, and then the samples were cooled to room temperature in a pure He flow. For

Received: August 5, 2010
Revised: February 26, 2011
Published: March 08, 2011

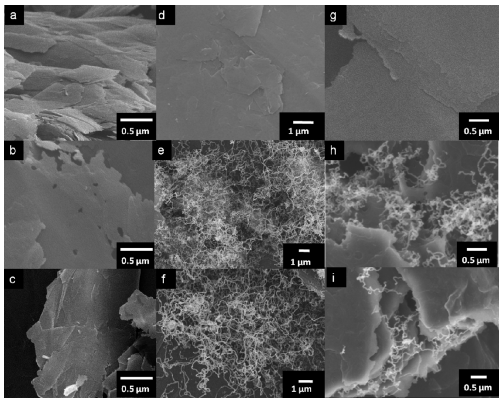

Figure 1. SEM images of (a) untreated as-received graphite. Graphite after oxidation pre-treatments by (b) oxygen oxidation and (c) acid treatment. (d, g) no CNTs found on untreated graphite after the CVD reaction of (e, h) dense CNTs on the graphite surface after oxygen oxidation pretreatent followed by the CVD reaction and (f, i) dense CNTs on the graphite surface after acid pretreatment followed by CVD processing.

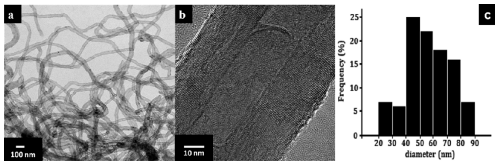

Figure 2. Typical TEM micrographs (a, b) of the produced carbon nanotubes on defect-rich graphite. (c) Diameter distribution of the as-grown CNTs on oxygen treated graphite.

a typical run, the sample size (pristine flake graphite or post-treated ones) is about 100 mg in a quartz reactor (diameter 10 mm, length 25 cm). For quantifying the amount of amorphous carbon and CNTs, we also performed the CVD experiments in situ in a TGA chamber, in which it is easy to monitor the weight gain from the cracking of ethylene and also to characterize the proportion of CNTs and amorphous carbons by the slow oxidation.[10,11] After the growing reaction of CNTs, the growth yield estimated by TGA measurements is about 9.32 mg CNT soot for 30 min reaction time. The weight percentage of CNTs calculated by TGA measurements is about 45% of the total CNT soot, so the synthesis yield is about 4.19 wt % or 8.38×10^{-2} g for 1 g of post-treated graphite per hour. Raman scattering measurements were conducted on a Jobin-Yvon T64000 spectrometer using a 532.2 nm excitation laser.

In Figure 1a the pristine graphite flakes are imaged using SEM. In Figure 1b,c the graphite after oxygen oxidation and acid oxidation treatments respectively are shown. The samples after post-treatments show porous features on their surface. After subjecting the samples to the thermal CVD reaction, no CNTs were observed on the pristine sample (Figure 1d,g). However, both treated samples showed apparently random and entangled fibers as can be seen from the SEM micrographs in Figure 1e,h and Figure 1f,i for oxygen and acid treated samples, respectively. TEM investigations show these structures to be multiwall CNTs. Typical examples are presented in Figure 2. The nanotube diameters range between 20 and 90 nm (mainly between 40 and 80 nm). EDS analysis shows only carbon and copper

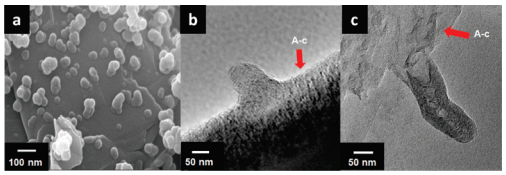

Figure 3. SEM image of (a) carbon nanobumps initially formed on the surface of the acid-treated flake graphite. TEM images of (b) a typical carbon nanobump and (c) an as-grown MWCNT with close-cap feature. Arrows in (b, c) indicate amorphous carbon (a−c) layer formed and covered on graphite surface.

signals; the latter is owing to the TEM sample holder (see Figure S1 in Supporting Information).

Further elemental analysis for original or treated graphites was required and monitored by TGA and ICP-MASS measurements. All of the graphite samples display only parts per million levels of metal or nonmetal elements (see Table S1 in Supporting Information). This level of noncarbon elements was described without remarkable effects for growing CNTs.[12,13] In addition, the CNT growth on defective graphite samples is particularly senstive to the carbon sources. Methane and ethylene are positive ones for growing CNTs on defected graphite; however, only amorphous carbons were obtained for alcohols and cyclohexane. This indicates that our post-treated methods did not introduce outcoming or exposure catalysts in the sublayers of post-treated graphite to contribute the growth of CNTs.

To gain insight into the growth mechanism behind this metal-free CVD route, we investigated treated samples after only a short thermal CVD exposure (<5 min). Figure 3a,b shows representative SEM and TEM micrographs from such samples. Typically after short CVD treatments the treated graphitic surfaces are covered with many bumps with diameters ranging between 40 and 80 nm, which is good agreement with that of the CNT obtained with longer reaction times. A typical close-up CNT that extrudes out from a layer of amorphous carbon covered graphite is shown in Figure 3c. The growth feature at the bottom position is like a self-assembly or lift-off model, which is unlike that of the as-known tip-growth or root-growth models. We did not observe any noncarbon elements inside the CNT. No differences between acid treated and oxygen treated samples were observed. Moreover, with longer reaction times in which the could CNT form, these nanobumps are not found. The data hints that defective sites are key to the formation of CNT. Previous studies indicate that dangling structures of carbons can catalytically decompose hydrocarbons.[12−14] Defective sites are good candidates to decompose the carbon source and lead to the formation of the nucleating nanobumps. Once these nanobumps have formed, whether from a lift-off process or self-assembly mechanism, CNT growth proceeds. Our previous studies point toward the self-assembly of CNTs on carbon black[13] and on bulk Au surfaces.[14] In this self-assembly process, a metastable carbon layer is deposited at high curvature positions, which allows easy formation of a hemispherical cap for growing CNTs.

For verifying our concepts, we used a laser-ablated HOPG as substrate to grow CNTs through ethylene CVD at 850 °C. SEM image of Figure 4a depicts typically defective features of laser-ablated HOPG. A close view inside the treated area shown in Figure 4b displaying various nanobumps after laser ablation, which is consistent with those of treated flake graphite. After the CVD process, it is not surprising to find that CNTs are densively

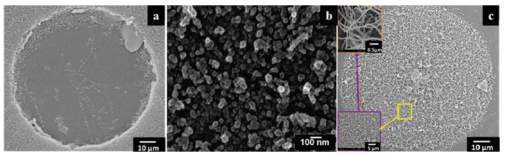

Figure 4. SEM images of (a) HOPG by laser abaltion and (b) a close-up image of (a) and (c) performed in CVD process at 850 °C in diluted ethylene (C_2H_4/He = 1/9) for 30 min. The lower-left (scale bar 5 μm) and upper-left (scale bar 0.5 μm) insets display close-up images of the marked area of as-grown CNTs on HOPG.

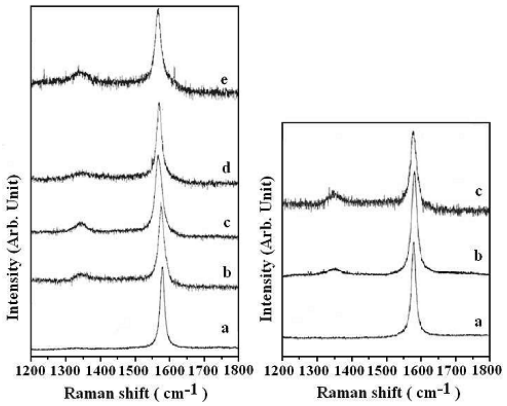

Figure 5. Left Panel: Raman spectra of (a) untreated graphite, (b) oxygen oxidized graphite, (c) acid-treated graphite, (d) as-grown CNTs on oxygen oxidized graphite, and (e) as-grown CNTs on acid-treated graphite. Right Panel: Raman spectra of (a) untreated HOPG, (b) laser-ablated HOPG, and (c) as-grown CNTs on laser-ablated HOPG.

grown in the treated area demonstrated in Figure 4c. Only the carbon signal was obtained by EDS analysis of pristine, laser-ablation and CNT-grown HOPG (see Figure S2 in Supporting Information).

In addition, Raman spectra can provide further information, although in this case it is limited because one cannot easily distinguish between the graphite support and the CNT. Nonetheless some information can be extracted. sp^2 carbon species typically show a response around 1580 cm^{-1} (G-band) arising from vibrations in the basal plane of the crystal and another feature around 1350 cm^{-1} (D-band) due to defects. In the left panel of Figure 5, typical Raman spectra for the samples are presented. Spectrum (a) shows a narrow G mode, and no D mode is observed. After oxidation treatments via oxygen (spectrum b) or acid (spectrum c) a clear D mode is observed and is indicative of defect formation. This is concomitant with the oxidation treatment etching the surface. After the CVD reaction, the D modes remain. Similar results were obtained for HOPG; Raman spectra are depicted in the right panel (spectra a−c) of Figure 5. The I_D/I_G ratios of laser-ablated and as-grown CNT samples are obsiously increasing.

To obtain further infromation of oxygenated functional groups (OFGs) on treated graphite, we performed titration analysis using the Boehm method.[15] The data shows an increase in carboxyl, lactone, and carbonyl groups for acid and oxidation treatments (see Table S2 in Supporting Information). However, the function of OFGs for growing CNTs is minor owing to their thermal stability at reaction temperature, 850 °C, and will completely decompose and leave only defective structures. This has been demonstrated in previous studies.[16,17]

The overall results are interesting and highlight that catalyst particles, either metallic on nonmetallic, are not a prerequisite for CNT formation. This is very much in keeping with Iijima's[18] pioneering work in which he grew MWCNTs from pure graphite electrodes via arc discharge without any catalyst addition.

Our findings show it is possible to grow carbon nanotubes directly on defect rich graphite via CVD. We show three activated routes to introduce surface defects: oxygen oxidation at elevated temperature, acid treatment, and laser ablation. We show that initially nanobumps form on the surface which act as nucleation centers for nanotube growth. Striking similarities to CNTs grown on carbon black and bulk Au suggest they grow through a self-assembly process. This approach can provide valuable implications for understnading the growth mechanism of CNTs via a metal-free CVD process.

■ ASSOCIATED CONTENT

Supporting Information. EDS results and ICP-MASS data (PDF). This material is available free of charge via the Internet at http://pubs.acs.org.

■ ACKNOWLEDGMENT

J.H.L. (NSC-98-2113-M-024-001, NSC-99-2113-M-024-001-MY2) and H.W.C. (NSC-98-2113-M-110-006-MY3) express their sincere appreciation to the National Science Council of Taiwan for supporting this study financially. M.H.R. thanks the EU (ECEMP) and the Freistaat Sachsen. A.B. thanks the Alexander von Humboldt Foundation.

■ REFERENCES

(1) Hou, P. H.; Liu, C.; Cheng, H. M. *Carbon* **2008**, *46*, 2003.
(2) Cho, H. G.; Kim, S. W.; Lim, H. J.; Yun, C. H.; Lee, H. S.; Park, C. R. *Carbon* **2009**, *47*, 3544.
(3) Dementev, N; Osswald, S.; Gogotsi, Y.; Borguet, E. *J. Mater. Chem.* **2009**, *19*, 7904.
(4) Liu, B.; Ren, W.; Gao, L.; Li, S.; Pei, S.; Liu, C.; Jiang, C. B.; Cheng, H. M. *J. Am. Chem. Soc.* **2009**, *131*, 2082.
(5) Huang, S.; Cai, Q.; Chen, J.; Qian, Y.; Zhang, L. *J. Am. Chem. Soc.* **2009**, *131*, 2094.
(6) Takagi, D.; Homma, Y.; Hibino, H.; Suzuki, S.; Kobayashi, Y. *Nano Lett.* **2006**, *6*, 2642.
(7) Takagi, D.; Kobayashi, Y.; Hibino, H.; Homma, Y. *J. Am. Chem. Soc.* **2009**, *131*, 6922.
(8) Takagi, D.; Kobayashi, Y.; Hibino, H.; Suzuki, S.; Homma, Y. *Nano Lett.* **2008**, *8*, 832.
(9) Liu, H.; Takagi, D.; Chiashi, S.; Homma, Y. *Carbon* **2010**, *48*, 114.
(10) Bom, D.; Andrews, R.; Jacques, D.; Anthony, J.; Chen, B.; Meier, M. S.; Selegue, J. P. *Nano Lett.* **2002**, *2*, 615.
(11) Mckee, G. S. B.; Vecchio, K. S. *J. Phys. Chem.* **2006**, *110*, 179.
(12) Muradov, N; Smith, F; Raissi, A. T. *Catal. Today* **2005**, *102−103*, 225.
(13) Lin, J. H.; Chen, C. S.; Ma, H. L.; Hsu, C. Y.; Chen, H. W. *Carbon* **2008**, *46*, 1619.
(14) Lin, J. H.; Chen, C. S.; Rümmeli, M. H.; Zeng, Z. Y. *Nanoscale* **2010**, *2*, 2835.
(15) Boehm, H. P. *Carbon* **1994**, *32*, 759.
(16) Lin, J. H.; Chen, H. W.; Wang, K. T.; Liaw, F. H. *J. Mater. Chem.* **1998**, *8*, 2169.
(17) Gorgulho, H. F.; Mesquita, J. P.; Gonçalves, F.; Pereira, M. F. R.; Figueiredo, J. L. *Carbon* **2008**, *46*, 1544.
(18) Iijima, S. *Nature* **1991**, *354*, 56.